

## Supporting Information:

# Scalable Parallel Algorithm for Graph Neural Network Interatomic Potentials in Molecular Dynamics Simulations

Yutack Park,<sup>†</sup> Jaesun Kim,<sup>†</sup> Seungwoo Hwang,<sup>†</sup> and Seungwu Han<sup>\*,†,‡</sup>

<sup>†</sup> *Department of Materials Science and Engineering and Research Institute of Advanced  
Materials, Seoul National University, Seoul 08826, Korea*

<sup>‡</sup> *Korea Institute for Advanced Study, Seoul 02455, Korea*

E-mail: [hansw@snu.ac.kr](mailto:hansw@snu.ac.kr)

## GPU utilization with respect to the number of atoms

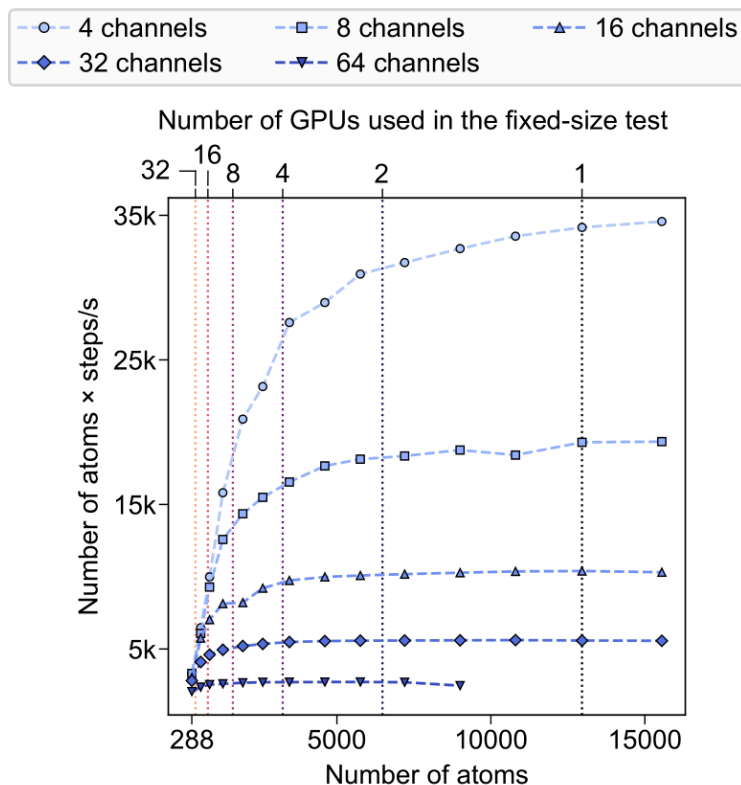


**Figure S1.** Single GPU utilization curve of models with four message-passing layers and 4, 8, 16, 32, and 64 channels. The dotted lines indicate the number of atoms used in the fixed-size test.

Figure S1 shows how the different number of channels and the number of atoms affects GPU utilization. The y-axis, the number of atoms multiplied by timesteps per second, indicates the amount of work (number of atoms multiplied by MD step) a GPU can yield in a unit of time (second). A plateau in this figure signifies full GPU utilization, achieved when a sufficient number of atoms is allocated. Conversely, a ballistic region observed at lower atom counts represents the GPU is in a suboptimal state. Notably, as the number of channels decreases, a greater number of atoms is needed to transition from this suboptimal state to the fully utilized state.

## Single GPU performance of SevenNet and NequIP

Considering the original NequIP is the baseline of our implementation, we compare a single GPU performance of SevenNet and NequIP. We use the same model hyperparameters of 32 channels, 4 message-passing layers, a maximum degree of representation ( $l_{\max}$ ) of 3, and a cutoff radius of 4.0 Å. The same benchmark script used in the scaled-size tests section is utilized. The benchmark runs span 210 MD steps, and we measure wall-clock time over the final 100 steps. The benchmark system involves alpha-quartz  $\text{SiO}_2$  containing 4,608 atoms. SevenNet, and NequIP achieved 1.99, and 1.12 timesteps per second, respectively.

For NequIP, we used the original implementation for training<sup>1</sup> and inference<sup>2</sup>. The SevenNet pair style is compiled with LAMMPS (23 Jun 2022 - Update 4), while the NequIP pair style uses a different version of LAMMPS (29 Sep 2021 - Update 2). Both pair styles utilize LibTorch from PyTorch/1.12.1. The compilation was done with nvcc compiler from CUDA/11.4, and gcc/8.3.0. The benchmarks are conducted on NVIDIA A100 80GB GPU in the KISTI Neuron cluster.

## Scaling of SevenNet and MACE

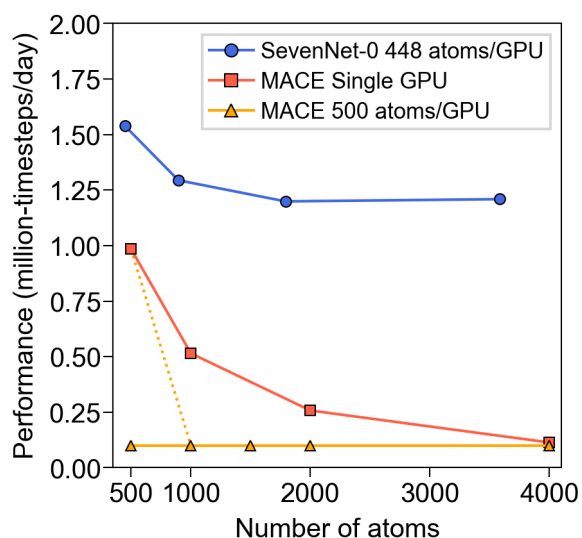


**Figure S2.** Weak-scaling performance of SevenNet-0 and MACE-MP-0<sup>3</sup>. The blue circles represent the performance of SevenNet in 448-atom amorphous Si<sub>3</sub>N<sub>4</sub>, from single to 8 GPUs. For MACE-MP-0, the red rectangle and yellow triangles indicate single-GPU and multi-GPU performance, respectively, measured with the high-entropy alloy system (500 atoms per GPU). The dashed line signifies the transition to multi-GPU in MACE. It is seen that the multi-GPU implementation of MACE becomes favorable only for very large-scale simulations due to significant additional costs. In contrast, SevenNet-0 well maintains the parallel efficiency regardless of the GPU number.

## References

- (1) Batzner, S.; Musaelian, A.; Sun, L.; Geiger, M.; Mailoa, J. P.; Kornbluth, M.; Molinari, N.; Smidt, T. E.; Kozinsky, B. *NequIP*, v0.5.6; Github:<https://github.com/mir-group/nequip> (accessed 2024-04-08).

(2) Batzner, S.; Musaelian, A.; Sun, L.; Geiger, M.; Mailoa, J. P.; Kornbluth, M.; Molinari, N.; Smidt, T. E.; Kozinsky, B. *Pair-Nequip*, v0.5.2; Github:[https://github.com/mir-group/pair\\_nequip](https://github.com/mir-group/pair_nequip) (accessed 2024-04-08).

(3) Batatia, I.; Benner, P.; Chiang, Y.; Elena, A. M.; Kovács, D. P.; Riebesell, J.; Advincula, X. R.; Asta, M.; Baldwin, W. J.; Bernstein, N.; Bhowmik, A.; Blau, S. M.; Cărare, V.; Darby, J. P.; De, S.; Pia, F. D.; Deringer, V. L.; Elijošius, R.; ElMachachi, Z.; Fako, E.; Ferrari, A. C.; Genreith-Schriever, A.; George, J.; Goodall, R.E. A.; Grey, C. P.; Han, S.; Handley, W.; Heenen, H. H.; Hermansson, K.; Holm, C.; Jaafar, J.; Hofmann, S.; Jakob, K. S.; Jung, H.; Kapil, V.; Kaplan, A. D.; Karimitari, N.; Kroupa, N.; Kullgren, J.; Kuner, M. C.; Kuryla, D.; Liepuoniute, G.; Margraf, J. T.; Magdău, I.-B.; Michaelides, A.; Moore, J. H.; Naik, A. A.; Niblett, S. P.; Norwood, S. W.; O'Neill, N.; Ortner, C.; Persson, K. A.; Reuter, K.; Rosen, A. S.; Schaaf, L. L.; Schran, C.; Sivonxay, E.; Stenczel, T. K.; Svahn, V.; Sutton, C.; Oord, C.v. d.; Varga-Umbrich, E.; Vegge, T.; Vondrák, M.; Wang, Y.; Witt, W. C.; Zills, F.; Csányi, G. A foundation model for atomistic materials chemistry. *arXiv* **2023**, arXiv:2401.00096. <https://arxiv.org/abs/2401.00096>  
arXiv.org ePrint archive